The ^{111m}Cd Nuclear Quadrupole Interaction in $CdCl_2$ and its Monohydrate *

Th. Fraenzke and T. Butz

Physik-Department, Technische Universität München, Garching, Germany

A. Lerf

Walther-Meißner-Institut für Tieftemperaturforschung der Bayerischen Akademie der Wissenschaften, Garching, Germany

Z. Naturforsch. **47a**, 89–95 (1992); received August 6, 1991

The ^{111m}Cd nuclear quadrupole interaction in $CdCl_2$ and $CdCl_2 \cdot H_2O$ was determined in the temperature range from 77 K to 783 K and 363 K, respectively, by time differential perturbed angular correlation. In addition, both the crystallization of the monohydrate from solution and its dehydration were monitored in situ.

1. Introduction

The nuclear quadrupole interaction (NQI) in layered transition metal dichalcogenides usually decreases linearly with increasing temperature [1]. This behaviour was attributed to anisotropic lattice vibrations and is the two-dimensional analog of the $T^{3/2}$-power law in three dimensions [2]. In order to investigate the origin of this linear power law further we choose another layered compound, namely the chloride of the post-transition metal Cd. Since there is no suitable isotope for NQI studies by NMR or NQR, we used the time differential perturbed angular correlation (TDPAC) of γ-rays of ^{111m}Cd ($T_{1/2} = 48.6$ min). Since $CdCl_2$ is hygroscopic, we studied in addition in detail the NQI of its monohydrate.

2. Experimental

The TDPAC experiments were performed with a conventional 4-detector spectrometer and with the Munich high efficiency TDPAC setup [3] on the 150 keV – 245 keV cascade. CdO with natural isotopic abundance was irradiated at the Forschungsreaktor München with a thermal neutron flux of $1.2 \cdot 10^{13}$ n/cm^2 s for 30 min and subsequently dissolved in 3 N HCl. The monohydrate was obtained by evaporating the solution to dryness at temperatures below 333 K (sometimes with inactive $CdCl_2 \cdot H_2O$ added as seeds). The crystallization was also monitored in situ. After completion of the TDPAC experiments we checked the sample by Debye-Scherrer X-ray diffraction. $CdCl_2$ was prepared in two ways: (i) 5 mg of neutron irradiated Cd metal was added to 67.9 mg $CdCl_2$ and heated to 903 K for 15 min, well above the melting point; subsequently, it was cooled to room temperature in 10–15 min. Here, the excess Cd segregates during cooling. (ii) the monohydrate, as prepared above, was heated to 453 K in vacuum in order to achieve complete dehydration. The dehydration process was monitored in situ.

* Presented at the XIth International Symposium on Nuclear Quadrupole Resonance Spectroscopy, London, United Kingdom, July 15–19, 1991.

Reprint requests to Dr. T. Butz, Physik-Department, Technische Universität München, W-8046 Garching bei München.

3. Results

3.1 The Anhydrate

First, a mixture of neutron irradiated Cd metal (12.5 at%) and inactive $CdCl_2$ was investigated. At this composition, the melting point depression is largest. In the melt, an unperturbed correlation was observed with an upper limit for the exponential decay constant of $\lambda \leqq 0.2\ \mu s^{-1}$. The melting point was determined in two ways: (i) the TDPAC spectra changed abruptly from an unperturbed correlation to a strongly perturbed correlation between 783 K and 793 K; (ii) the solidification of an inactively prepared sample was monitored optically with a bore hole furnace equipped with a prisma: the colour changed from brown in the melt to grey in the solid at 787 K; upon heating, the colour changed at 783 K. This melting

0932-0784 / 92 / 0100-0089 $ 01.30/0. – Please order a reprint rather than making your own copy.

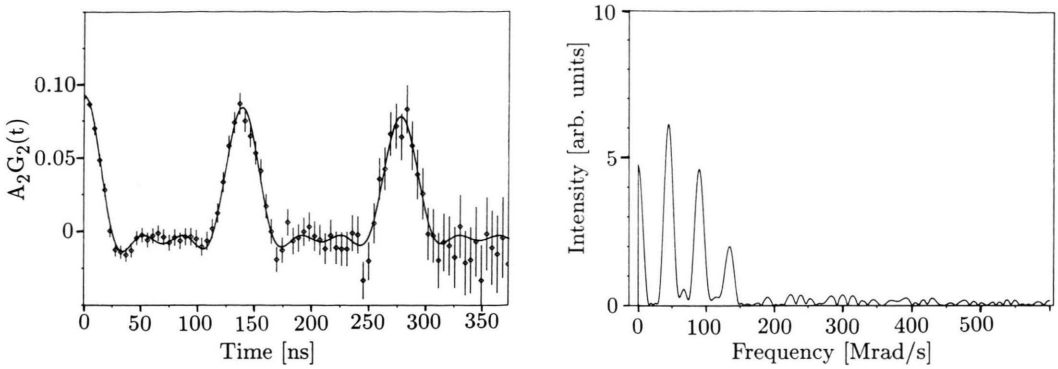

Fig. 1. TDPAC spectrum for the ^{111m}Cd NQI in $CdCl_2$ at 297 K (left) and its Fourier transform (right).

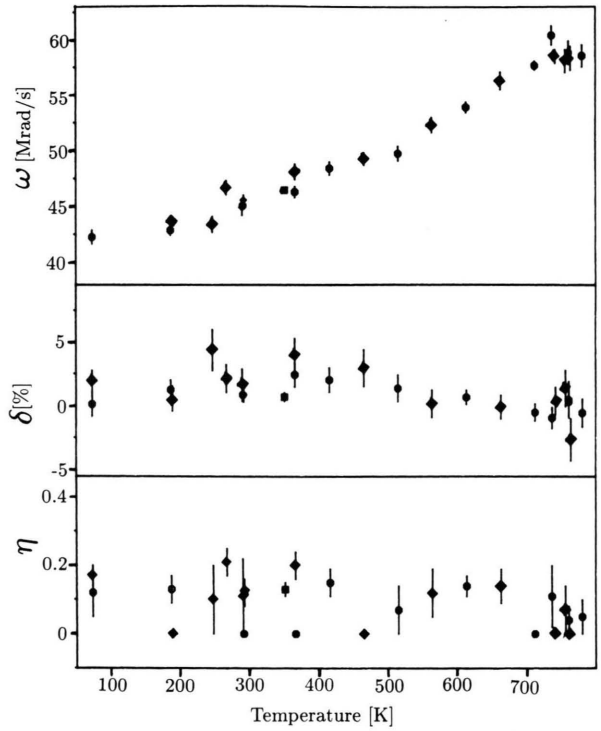

Fig. 2. Precession frequency ω, frequency distribution (Lorentzian) δ, and asymmetry parameter η versus temperature for the ^{111m}Cd NQI in $CdCl_2$.

point is somewhat low compared to the literature value of 803 K [4]. We believe that our $CdCl_2$ contained small amounts of water. This would lower the melting point drastically [4]. Another indication for trace amounts of water in our sample is the fact that our melt was not deeply black, as expected, but brown. According to Corbett et al. [5] this change of colour is due to O^{2-} impurities in samples containing small amounts of water.

Upon solidification, two different NQI's were observed: the signal of $CdCl_2$ and a minority signal of bulk Cd metal. Normally, the fraction of the bulk Cd metal signal was about 15–25%. From this we conclude that keeping the melt at 903 K (well above the melting point) for 15 min is quite sufficient to distribute the ^{111m}Cd homogeneously over the entire sample. We found that lowering the temperature to close above the melting point did not guarantee a homogeneous doping with ^{111m}Cd within 15 min. Due to the short halflife of ^{111m}Cd of 49 min we could not afford longer mixing times. Furthermore, upon solidification a segregation into bulk Cd metal and $CdCl_2$ takes place without other detectable species. The temperature dependence of the bulk Cd metal signal was identical to that reported earlier [6]. Since the temperature dependence of the $CdCl_2$ signal was identical to that obtained for $CdCl_2$ prepared by method (ii) we shall present both results together.

A typical TDPAC spectrum of $CdCl_2$ at 297 K is shown in Fig. 1 (left) together with its Fourier transform (right). The NQI has axial symmetry and there is only a very small damping (line-broadening). Over the entire temperature range from 77 K up to 793 K the asymmetry parameter η was rather small and often compatible with zero. The damping, assumed Lorentzian, was always below 2.5%. The precession frequency ω increased from 42.3 (6) Mrad/s at 77 K to about 60 (1) Mrad/s at 748–793 K. Representative results of the least squares fitting analysis are listed in Table 1 and all results are summarized in Figure 2. The quadrupole frequency $\nu_Q = e^2 q Q/h$, with $eq = V_{zz}$ denoting the largest component of the electric field

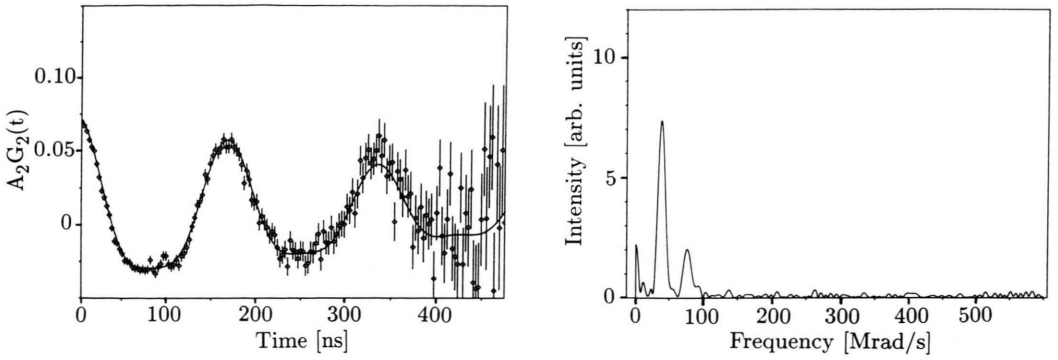

Fig. 3. TDPAC spectrum for the ^{111m}Cd NQI in $CdCl_2 \cdot H_2O$ at 298 K (left) and its Fourier transform (right).

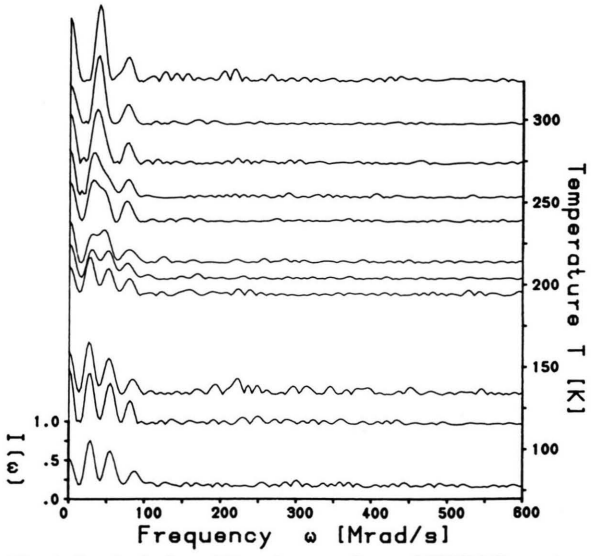

Fig. 4. Stacked plot of Fourier transformed TDPAC spectra showing the variation of the precession frequency and the asymmetry parameter with temperature.

Table 1. Precession frequency ω, frequency distribution (Lorentzian) δ, and asymmetry parameter η for the ^{111m}Cd NQI in $CdCl_2$.

T[K]	ω [Mrad/s]	δ [%]	η
77	42.3 (6)	0.1 (9)	0.12 (7)
192	42.9 (4)	1.3 (8)	0.13 (4)
297	45.3 (2)	0.9 (4)	0.00 (–)
353	46.4 (2)	0.7 (3)	0.13 (2)
373	46.3 (5)	2.5 (10)	0.00 (–)
423	48.4 (6)	2.1 (10)	0.15 (4)
523	49.8 (7)	1.4 (10)	0.06 (7)
623	54.0 (5)	0.7 (6)	0.14 (3)
723	57.7 (4)	−0.5 (7)	0.00 (–)
748	60.4 (9)	−0.9 (8)	0.11 (9)
773	58.9 (10)	0.4 (12)	0.04 (4)
793	58.6 (10)	−0.5 (11)	0.05 (5)

Quantities where no error limits are quoted were not treated as an adjustable parameter.

gradient (EFG) tensor, and eQ being the $I = 5/2$ state nuclear quadrupole moment, is related to the precession frequency by [7]:

$$\nu_Q = \frac{10\,\omega}{\sqrt{3}\,\alpha\,\pi\,\sin(\arccos(\beta)/3)} \tag{1}$$

with $\alpha = \sqrt{28(3+\eta^2)/3}$ and $\beta = 80(1-\eta^2)/\alpha^3$.

For $\eta = 0$ we simply have $\nu_Q = \frac{10}{3\pi}\,\omega = 1.061\,\omega$.

3.2 The Monohydrate

A typical TDPAC spectrum of $CdCl_2 \cdot H_2O$ at 298 K is shown in Fig. 3 (left) together with its Fourier transform (right). It is immediately clear that the asymmetry parameter is close to unity. Contrary to the anhydrate, both the precession frequency ω and the asymmetry parameter η vary drastically with temperature. At 77 K we have $\omega = 28.2\,(6)$ Mrad/s and $\eta = 0.17\,(6)$ whereas close to the dehydration temperature of 323 K we have $\omega = 38.8\,(5)$ Mrad/s and $\eta = 1$. A stacked plot of Fourier transformed TDPAC data versus temperature is shown in Figure 4. All results of the least squares fitting analysis are summarized in Table 2 and shown in Figure 5. Note that the increase of ω with increasing temperature is entirely due to the increase of the asymmetry parameter despite the decrease of V_{zz} (cf. (1) and see Fig. 8 top).

3.3 Higher Hydrates of $CdCl_2$

Our attempts to prepare the 2.5-hydrate and the 4-hydrate of $CdCl_2$ were unsuccessful. The higher hydrates exist only over a limited range of temperature and are rather unstable against dehydration. Never-

theless, we obtained twice a TDPAC spectrum at 300 K which was entirely different from that of the monohydrate. Such a spectrum is shown in Fig. 6 (left) together with its Fourier transform (right). The precession frequency is $\omega = 144.5\,(12)$ Mrad/s with $\eta = 0.57\,(1)$ at 298 K and 145.7 (15) Mrad/s with $\eta = 0.56\,(1)$ at 261 K. We made no attempts to determine the crystal structure by X-ray diffraction because of the limited stability of the product. Since the 4-hydrate is completely unstable at room temperature we speculate that this sample was in fact the 2.5-hydrate.

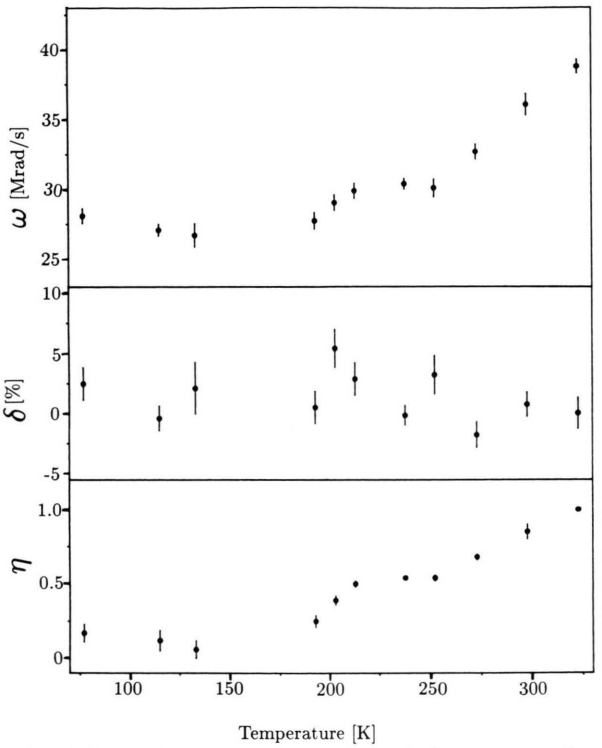

Fig. 5. Precession frequency ω, quadrupole frequency ν_Q, frequency distribution (Lorentzian) δ, and asymmetry parameter η versus temperature for the ^{111m}Cd NQI in $CdCl_2 \cdot H_2O$.

3.4 Crystallization of $CdCl_2 \cdot H_2O$ from Solution

Using the Munich TDPAC setup we monitored in situ the crystallization of the monohydrate from solution at 298 K under mild pumping. Whereas the ^{111m}Cd in solution exhibits an unperturbed correlation due to the rapid tumbling motion of the small molecule, crystallized $CdCl_2 \cdot H_2O$ exhibits a static signal as described in Section 3.2. Spectra taken every 10–15 min showed that after an induction period of about 25 min during which we probably saturated the solution the crystallization took place continuously until it was completed between 100 and 150 min. We

Table 2. Precession frequency ω, frequency distribution (Lorentzian) δ, and asymmetry parameter η for the ^{111m}Cd NQI in $CdCl_2 \cdot H_2O$.

T[K]	ω [Mrad/s]	δ [%]	η
77	28.2 (6)	2.5 (13)	0.17 (6)
115	27.1 (4)	−0.4 (10)	0.12 (7)
133	26.7 (9)	2.1 (22)	0.06 (6)
193	27.7 (6)	0.5 (14)	0.25 (4)
203	29.0 (6)	5.4 (16)	0.39 (3)
213	29.9 (6)	2.9 (14)	0.50 (2)
238	30.4 (4)	−0.1 (8)	0.54 (1)
252	30.1 (7)	3.2 (16)	0.54 (2)
273	32.7 (6)	−1.8 (11)	0.68 (2)
298	36.1 (8)	0.8 (10)	0.87 (5)
298	35.2 (3)	2.5 (6)	0.86 (2)
323	38.8 (5)	0.1 (13)	1.00 (–)

Quantities where no error limits are quoted were not treated as adjustable parameters.

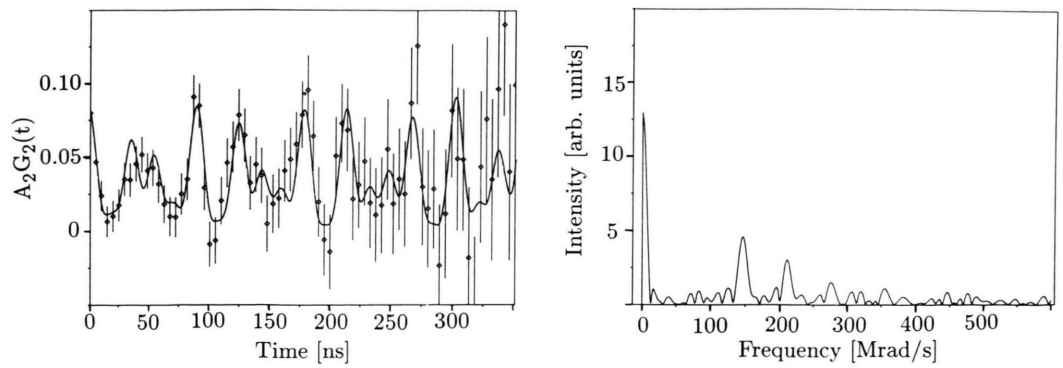

Fig. 6. TDPAC spectrum fo the ^{111m}Cd NQI of a higher hydrate of $CdCl_2$ (2.5-hydrate?) at 298 K (left) and its Fourier transform (right).

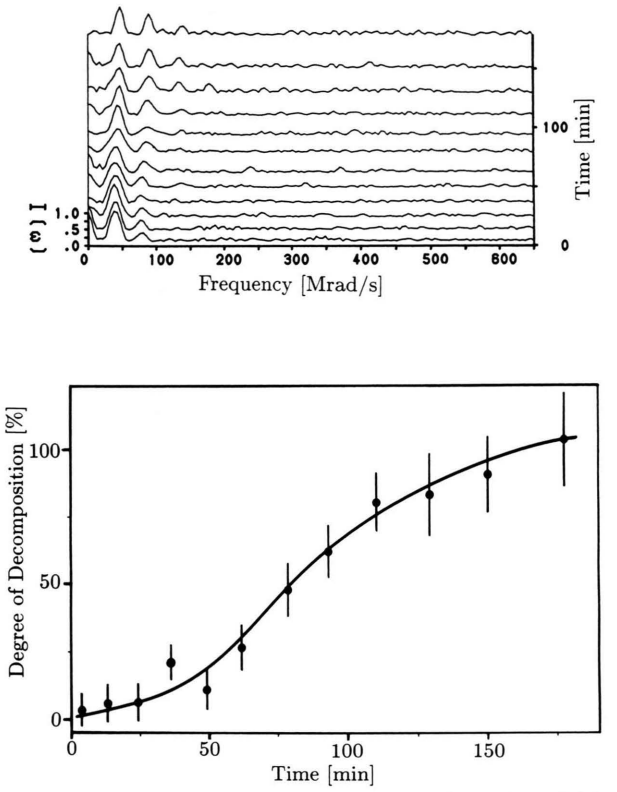

Fig. 7. *Top:* Stacked plot of Fourier transformed TDPAC spectra taken during in situ monitoring of thermal dehydration of $CdCl_2 \cdot H_2O$. *Bottom:* Fraction of dehydrated $CdCl_2$ versus time.

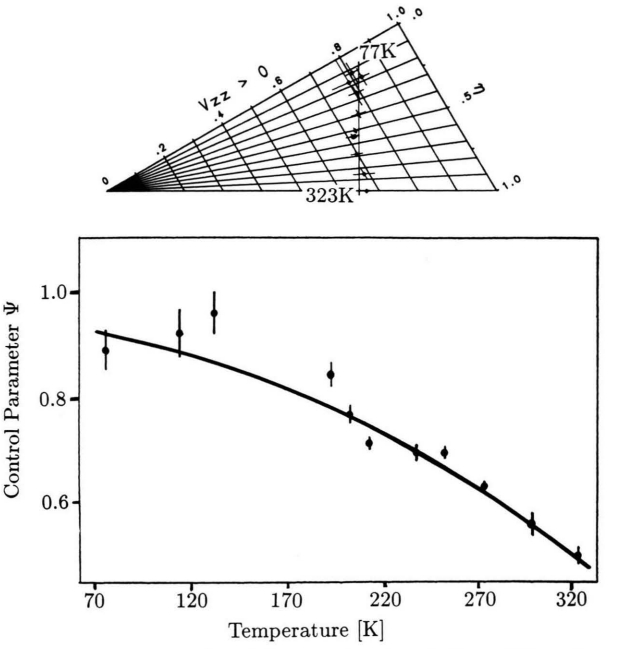

Fig. 8. *Top:* Czjzek-plot of the correlated variation of V_{zz} and η for the ^{111m}Cd NQI in $CdCl_2 \cdot H_2O$. *Bottom:* Control parameter describing the interchain coupling strength in $CdCl_2 \cdot H_2O$ versus temperature.

did not observe any signal which could be attributed to other species than the monohydrate during crystallization.

3.5 Dehydration of the Monohydrate

Using the Munich TDPAC setup we monitored in situ the dehydration of the monohydrate in a sealed, heated ampoule. We first heated the sample to 333 K without any detectable dehydration. We then increased the temperature to 353 K in small steps. The water was allowed to condense at the cold end of the ampoule. Spectra taken every 10–15 min showed that the dehydration took place progressively and was completed after about 150–180 min (see Figure 7). Since the reaction was not carried out isothermally we shall not attempt a quantitative analysis. Our main purpose is to show that such processes can be studied with very short data collection times.

4. Discussion

4.1 The Anhydrate

First, we shall discuss the unperturbed correlation of the $Cd/CdCl_2$ melt. The relaxation rate λ is related to the reorientational correlation time τ_c in the Abragam-Pound limit by [8]:

$$\lambda = \frac{14}{5} \langle \omega^2 \rangle \tau_c \quad \text{for} \quad I = 5/2. \tag{2}$$

We found experimentally that $\lambda \leqq 0.2\,\mu s^{-1}$. The reorientational correlation time is related to the volume of the molecule by the Stokes-Einstein relationship (spherical rotor):

$$\tau_c = \frac{V\bar{\eta}}{k_B T} \quad \text{with} \quad \bar{\eta} \text{ denoting the viscosity.} \tag{3}$$

(We use a bar over $\bar{\eta}$ in order to distinguish it from the asymmetry parameter η).

Assuming $\omega \sim 50$ Mrad/s for the melt, as for solid $CdCl_2$ close to the melting point, and a viscosity of $\bar{\eta} = 0.0211$ P at 923 K [4] we obtain an upper limit for the radius of the molecule in the melt of $r \leqq 3.5$ Å. Unfortunately, this upper limit does not allow to distinguish between the proposed Cd_2^{2+} [9] and Cd_2Cl_2

[5, 10] in the melt. In any case, such species are no longer present below the melting point since no other signal than that of bulk Cd metal and of $CdCl_2$ were ever observed.

Our result for the NQI at room temperature is in good agreement with that reported previously by Barfuß et al. [11]. Attempts by these authors to use ^{111}In, which decays via electron capture to ^{111}Cd, as a TDPAC probe – it would be much more convenient due to the longer halflife – failed, as did the attempts by Damonte et al. [12]. Apparently, either it is not possible to dope $CdCl_2$ with ^{111}In substitutionally, or after-effects associated with the electron capture process render this probe useless for this purpose.

Next, we discuss the temperature variation of V_{zz}. An increase of V_{zz} with increasing temperature is somewhat unexpected for a layered material when compared with e.g. TaS_2 [1]. Therefore, we believe that lattice vibrations are not the dominant source for the temperature variation of V_{zz}. An interesting idea has been put forward by Barfuß et al. [13] and Witthuhn [14] for ^{111}Cd in Te where a similar increase of V_{zz} with temperature was correlated with the increase of the carrier density. If one plots the logarithm of ω versus reciprocal temperature one can indeed approximate the variation of $\ln \omega$ by a straight line in the high temperature region yielding a band gap of about 0.25 eV. However, this value is undoubtedly too low (absorption edge: 5.03 eV [15]). Barfuß et al. [13] also observed that their activation energy was much lower than the band gap of Te. However, in their case they possibly determined the position of the impurity level Cd^{2+} in the band gap of Te whereas in our case we are not dealing with impurity atoms at all. Therefore, we believe that the increase of V_{zz} with increasing temperature is not due to an increase of the carrier density. Unfortunately, the lattice parameters of $CdCl_2$ as a function of temperature to our knowledge are not known yet. Therefore, no further conclusions can be drawn at present.

4.2 The Monohydrate

Haas and Shirley [16] reported the NQI of the 2.5-hydrate of $CdCl_2$ already in 1973. Incidentally, they quote the same NQI parameters for their sample as we observed for the monohydrate. From our X-ray analysis and from our in situ crystallization studies we are sure that our data are for the monohydrate. The only higher hydrate we eventually have observed was the 2.5-hydrate (see Section 3.3). Therefore, we believe that Haas and Shirley also had the monohydrate. An interesting feature of V_{zz} and η in the monohydrate is their rather strong temperature variation. However, the most striking feature of the temperature variation of V_{zz} and η becomes clear when plotted in the way proposed by Czjzek [17] which is the reduced version of a carthesian plot of V_{zz} versus e.g. V_{xx}, as discussed in [18]. In this plot (see Fig. 8), it is evident that V_{zz} and V_{xx} (or V_{yy}) are linearly correlated. Moreover, all data points lie on a vertical line in the Czjzek-Plot. This means that the total EFG-tensor can be decomposed into two tensors which are both axially symmetric and simultaneously diagonal:

$$V_{ij} = \begin{pmatrix} -1/2 & 0 & 0 \\ 0 & -1/2 & 0 \\ 0 & 0 & 1 \end{pmatrix} + \Psi \begin{pmatrix} -1/2 & 0 & 0 \\ 0 & 1 & 0 \\ 0 & 0 & -1/2 \end{pmatrix}. \quad (4)$$

The first tensor in (4) represents the contribution of the linear chains in $CdCl_2 \cdot H_2O$. The second tensor accounts for the interchain coupling with the control parameter Ψ describing the interchain coupling strength which is mediated by H-bonds. This identification is immediately obvious upon inspection of the crystal structure of $CdCl_2 \cdot H_2O$ [19]. Cd is surrounded by five Cl-atoms and one O-atom in an octahedral configuration. These octahedra are connected along the chain direction. There are two possibilities: (i) V_{zz} of the isolated chains points along the chain direction or (ii) V_{zz} is perpendicular to the chain direction and also perpendicular to the interchain coupling due to H-bonds. In the former case, Ψ would increase with increasing temperature, whereas in the latter case Ψ decreases. This latter choice seems more plausible because the hydrogen bonds are expected to weaken upon heating. Therefore we plotted Ψ for choice (ii) in Fig. 8 (bottom). Here, a single crystal study would help to clarify this ambiguity. It is interesting to note that η approaches unity at the decomposition temperature. We do not know whether this is accidental or not.

Acknowledgement

The continuous interest and support of Prof. Dr. G. M. Kalvius and his hospitality is gratefully acknowledged. It is a pleasure to thank Dr. S. Saibene and W. Tröger for their help. This work was supported by the Bundesministerium für Forschung und Technologie (03-KA1TUM), FRG. The reactor irradiations were performed at the Forschungsreaktor München.

[1] A. Lerf and T. Butz, Angew. Chem. Int. Ed. Engl. **26,** 110 (1987).
[2] D. R. Torgeson and F. Borsa, Phys. Rev. Lett. **37,** 956 (1976).
[3] T. Butz, S. Saibene, Th. Fraenzke, and M. Weber, Nucl. Instrum. Meth. **A 284,** 417 (1989).
[4] Gmelin's Handbook of Inorganic Chemistry, Cadmium, Verlag Chemie, Weinheim 1959.
[5] J. D. Corbett, W. J. Burkhard, and L. F. Druding, J. Amer. Chem. Soc. **83,** 76 (1961).
[6] J. Christiansen, P. Heubes, R. Keitel, W. Klinger, W. Loeffler, W. Sandner, and W. Witthuhn, Z. Phys. **B 24,** 177 (1976).
[7] E. Gerdau, F. Wolf, H. Winkler, and J. Braunsfurth, Proc. Roy. Soc. London **A 311,** 197 (1969).
[8] A. Abragam and R. V. Pound, Phys. Rev. **92,** 943 (1953).
[9] K. Grjotheim, F. Grönvold, and J. Krogh-Moe, J. Amer. Soc. **77,** 5824 (1955).
[10] G. Wirths, Z. Elektrochem. **43,** 486 (1937).
[11] H. Barfuß, G. Böhnlein, H. Hohenstein, W. Kreische, H. Niedrig, H. Appel, J. Raudies, and W.-G. Thies, Hyperf. Interact. **10,** 962 (1981); H. Barfuß, G. Böhnlein, H. Hohenstein, W. Kreische, H. Niedrig, H. Appel, R. Heidinger, J. Raudies, G. Then, and W.-G. Thies, Z. Phys. **B 47,** 99 (1982).
[12] L. C. Damonte, L. A. Mendoza-Zelis, A. G. Bibiloni, J. Desimoni, C. P. Massolo, and A. R. Lopez-Garcia, Hyperf. Interact. **30,** 57 (1986).
[13] H. Barfuß, G. Böhnlein, P. Freunek, R. Hofmann, H. Hohenstein, W. Kreische, H. Niedrig, A. Reimer, W. Keppner, and W. Körner, Hyperf. Interact. **9,** 235 (1981).
[14] W. Witthuhn, Hyperf. Interact. **24–26,** 547 (1985).
[15] V. Grasso and R. Mondio, in: Electronic Structure and Electronic Transitions in Layered Materials, V. Grasso (ed.), Reidel Publ. Company, Holland, Dordrecht 1986.
[16] H. Haas and D. A. Shirley, J. Chem. Phys. **58,** 3339 (1973).
[17] G. Czjzek, Hyperf. Interact. **14,** 184 (1984).
[18] T. Butz, Hyperf. Interact. **35,** 1037 (1987).
[19] H. Leligny and J. C. Monier, Acta Cryst. **B 30,** 305 (1974).